Polymer adsorption on reconstructed Au(001): A statistical description of P3HT by scanning tunneling microscopy and coarse-grained Monte Carlo simulations

S. Förster, E. Kohl, M. Ivanov, J. Gross, W. Widdra, and W. Janke

Citation: The Journal of Chemical Physics **141**, 164701 (2014); doi: 10.1063/1.4898382
View online: http://dx.doi.org/10.1063/1.4898382
View Table of Contents: http://scitation.aip.org/content/aip/journal/jcp/141/16?ver=pdfcov
Published by the AIP Publishing

Polymer adsorption on reconstructed Au(001): A statistical description of P3HT by scanning tunneling microscopy and coarse-grained Monte Carlo simulations

S. Förster,[1,a)] E. Kohl,[1] M. Ivanov,[2,b)] J. Gross,[2,c)] W. Widdra,[1,3,d)] and W. Janke[2,e)]
[1]*Institute of Physics, Martin-Luther-Universität Halle-Wittenberg, Halle, Germany*
[2]*Institut für Theoretische Physik, Universität Leipzig, Postfach 100 920, D-04009 Leipzig, Germany*
[3]*Max-Planck-Institut für Mikrostrukturphysik, Halle, Germany*

(Received 4 August 2014; accepted 6 October 2014; published online 22 October 2014)

We report on a combined theoretical and experimental characterization of isolated Poly(3-hexylthiophene) (P3HT) chains weakly adsorbed on a reconstructed Au(001) surface. The local chain conformations of *in situ* deposited P3HT molecules were investigated by means of scanning tunneling microscopy. For comparison, Monte Carlo simulations of the system were performed up to a maximum chain length of 60 monomer units. The dependence of the end-to-end distance and the radius of gyration on the polymer chain length shows a good agreement between experiment and Monte Carlo simulations using simple updates for short chains. © *2014 AIP Publishing LLC*. [http://dx.doi.org/10.1063/1.4898382]

I. INTRODUCTION

Regioregular Poly(3-hexylthiophene) (P3HT) is a very well studied conjugated polymer due to its interesting electronic and optical properties.[1–4] Recently P3HT has attracted attention for the use in donor/acceptor blends for photovoltaic applications.[5–7] Studies of P3HT on the microscopic level are of great importance for a fundamental understanding of the tuneability of electronic properties and their dependence on external constraints, e.g., the adsorption on electrode surfaces. Hence a number of experimental studies addressed for example the influence of structure formation by polymer self-assembly on ideal surfaces on the electronic properties of oligo- and polythiophenes.[8,9] Due to the complexity of these macromolecules, the experimental findings have not been supported with simulations so far, which in contrast is well-established for studies of small organic molecules. This study reports on an approach to combine the experimental observation of polymer chain conformations adsorbed on a metal surface with coarse-grained Monte Carlo simulations.

In a previous study it has been shown that two different adsorption behaviours can be observed for *in situ* deposited P3HT molecules on an Au(001) surface.[10] The polymer molecules adsorb either as weakly bonded random chains or as stronger interacting entities which locally lift the Au(001) reconstruction. The former random chain conformation is metastable at room temperature. It allows a molecular diffusion on the surface and is in the focus of the present work. We show that the weakly adsorbed P3HT molecules on Au(001) can be modelled using the coarse-grained model of Huang *et al.*[11] P3HT chains with a maximum length of 60 monomers were simulated in contact with an Au(001) surface and the end-to-end distance as well as the radius of gyration of the molecules were determined. These parameters are compared with experimentally obtained chain conformations of *in situ* deposited P3HT molecules on Au(001) as observed with scanning tunneling microscopy (STM).

This paper is organised as follows. In Sec. II, we first describe the experimental setup. Section III A explains the computer model and the simulations of studied system - polymer and surface. In Sec. IV, we present and discuss the results from the STM experiments and the computer simulations. We conclude our findings in Sec. V.

II. EXPERIMENTAL

The experiments were performed in an ultra-high vacuum (UHV) system operating at a base pressure of 1×10^{-10} mbar which houses a home-build high-temperature scanning tunneling microscope operating in a temperature range between 300 and 850 K. In addition to standard sample preparation facilities, the chamber is equipped with a modified *in situ* UHV electrospray deposition source (Molecularspray, UK).[12,13] A detailed description of the experimental setup is given elsewhere.[10]

The Au(001) single crystal substrate (Mateck, Germany) was cleaned by several cycles of Ar^+ ion sputtering and subsequent annealing to 550 K for 20 min. Cleanliness and long-range order of the Au(001) surface were verified by scanning tunneling microscopy. Electrochemically etched Pt/Ir tips were used in the STM measurements.

By using electrospray deposition regioregular P3HT molecules were deposited on an Au(001) single crystal surface. Commercial high-quality P3HT polymer ($(C_{10}H_{14}S)_n$, BASF Sepiolid^{TM} P200, BASF, Germany) has been used with a molecular weight (M_W) of ~19.5 kg/mol and a polydispersity index (PDI) of 1.9. The regioregularity of the polymer

a)Electronic mail: stefan.foerster@physik.uni-halle.de
b)Electronic mail: momchil@itp.uni-leipzig.de
c)Electronic mail: gross@itp.uni-leipzig.de
d)Electronic mail: wolf.widdra@physik.uni-halle.de
e)Electronic mail: janke@itp.uni-leipzig.de

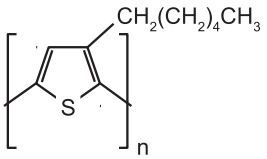

FIG. 1. The molecular structure of Poly(3-hexylthiophene-2,5-diyl) (P3HT).

has been determined to 80%. A sketch of the molecular structure is shown in Fig. 1. For the spray deposition the P3HT has been dissolved in a 3:1 mixture of trichloromethane and acetonitrile to a concentration of 10^{-5}. The acetonitrile was added to increase the polarity of the solvent which improves the electrospray process.

III. MODEL AND SIMULATION

A. Coarse-grained P3HT model

The coarse-grained (CG) formulation of the P3HT polymer from Huang *et al.*[11] was used as a basis for the computer simulations. The atomic structure of the polymer as well as the coarse-grained model consisting of three distinct types of particles $P1$, $P2$, and $P3$ are depicted in Fig. 2. Particles $P1$ represent thiophene rings along the backbone of the polymer and are positioned in the center of mass of the rings. Particles $P2$ and $P3$ represent the two parts of a side chain. They are centred around the first and the last three carbon atoms of a side chain, respectively. The parameters for this model were also taken from Ref. 11.

The intramolecular forces are modelled by four terms: anharmonic bond vibrations (U_{bond}), bending energy (U_{bending}), torsion energy (U_{torsion}), and interactions between non-bonded particles (U_{nb}). Bonds between coarse-grained particles are described by a potential of the form

$$U_{\text{bond}}(l) = \sum_{i=2}^{n} c_i (l - l_0)^i, \tag{1}$$

where n determines the number of the constants c_i, which is different for the three types of bonds. The equilibrium distance for the backbone particles is l_0(P1–P1) = 3.828 Å. Distances from backbone particle to the first side chain particle and between the two side chain particles are given by l_0(P1–P2) = 4.0717 Å and l_0(P2–P3) = 3.5379 Å, respectively. There is a total of 26 parameters for the bond length-potential taken from the supporting information for Ref. 11.

Angles between two bonds contribute to the total energy through the following bending potential

$$U_{\text{bending}}(\Theta) = \sum_{i=0}^{n} c_i (\Theta - \Theta_0)^i. \tag{2}$$

The backbone bending potential between three $P1$ particles is symmetrical around 180° with two distinct minima at ∼165° and ∼195°. Very similar to that is the angle between the side chain bonds bound by the particles P1–P2–P3. It is symmetrical around 180° with minima at ∼160° and ∼200°. The angle between P1–P1–P2 is symmetrical around its minimum at 122°, while the bending potential between P2–P1–P1 is minimal at 83°. Again, the constants c_i and their number n are different for the four combinations. There are 42 parameters in total describing the bending potential.

A torsion angle is given by the angle between the two normal vectors of two planes. One plane would include points A, B, and C, while the other plane includes points B, C, and D. The torsion-angle potential for the polymer model is parametrized as

$$U_{\text{torsion}}(\Phi) = \sum_{i=0}^{n} c_i \cos^i(\Phi), \tag{3}$$

and is plotted in Fig. 3, with 24 different constants c_i depending on the combination of particles. The torsion potential keeps the backbone particles P1 planar, while the side chains can slightly move out of the plane. In particular there are two minima in the potential of the side chains. One where the side chains point in opposite directions as depicted in Fig. 2, corresponding to a torsion angle of $\Phi = 180°$, and

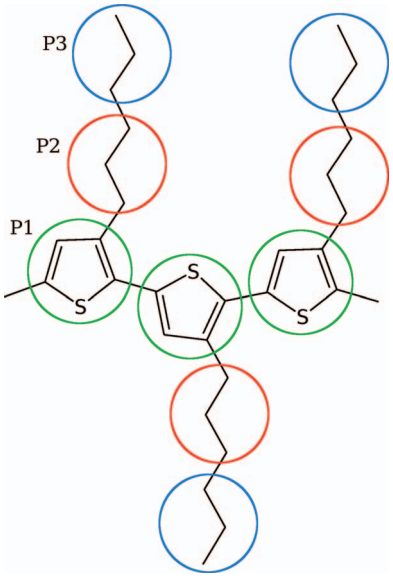

FIG. 2. Two-dimensional representation of a poly(3-hexylthiophene) chain with overlaying coarse-grained particles: P1 is positioned at the center of mass of the thiophene ring. P2 and P3 each surround three carbon atoms of the side chain methyl group.

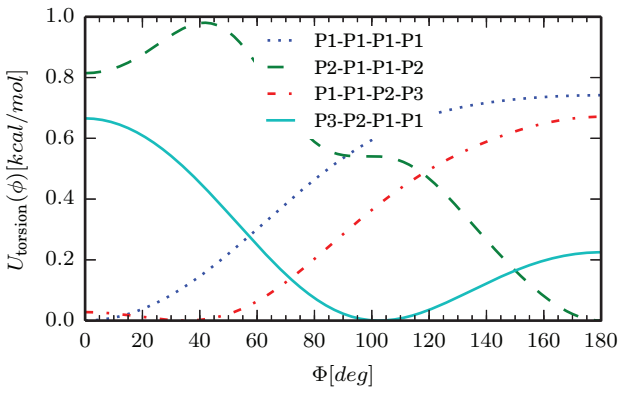

FIG. 3. Torsion-angle potential for the four possible particle combinations.

another minimum position with a slightly higher energy at $\Phi = 0°$, where neighbouring side chains point in the same direction, corresponding to the *trans* and *cis* conformations, respectively. Additionally to the proper torsion potential for chains of connected particles, there is also an improper torsion between non-connected particles P1–P2–P1–P1 with five parameters.

Finally, in addition to the already described potentials there is a contribution to the total energy from the interactions between non-bonded particles as well. These include Lennard-Jones like as well as Coulomb interactions and are given in form of a numerical table together with the values of the 97 parameters of the bonded potentials in the supporting information for Ref. 11.

B. Coarse-grained surface representation

The Au(001) surface is known to form a quasi-hexagonal reconstruction at the vacuum interface.[14] The height modulations of the atoms of the top-most hexagonal layer (e.g., see Fig. 1 in Ref. 14) induce a stripe-like patterning of the substrate terraces. Due to the high level of complexity a detailed theoretical description of the surface reconstruction is still lacking. However, when studying particle interaction with a surface, Steele[15] argues that variations of the position of the interacting particle over the unit cell of the surface leads to differences in the effective potential. Since this difference is only observable at very small distances from the surface this effect has been neglected in the simulations, because of the size of the coarse-grained particles used here. This allows for a coarse-graining of the surface as well.

The simplest approach is to use a wall-like potential

$$U_{\text{surf,9-3}}(z) = \frac{2\pi\epsilon\rho\sigma^3}{3}\left[\frac{2}{15}\left(\frac{\sigma}{z}\right)^9 - \left(\frac{\sigma}{z}\right)^3\right]. \quad (4)$$

Here z is the distance from the surface and ρ is the atom number density of the given material. It can be obtained by integrating over the $z < 0$ half-space and assuming a 12–6 Lennard-Jones interaction of a CG particle with every space element of the substrate. This potential, however, underestimates the distance of adsorbed particles to the surface. An improved surface potential was proposed by Hentschke.[16] Instead of integrating over the entire z-half-space, integration is performed over layers of the surface, giving the potential

$$U_{\text{surf,10-4}}(z,n) = 2\pi\epsilon\rho\Delta z\sigma^2 \times\left[\frac{2}{5}\left(\frac{\sigma}{z+n\Delta z}\right)^{10} - \left(\frac{\sigma}{z+n\Delta z}\right)^4\right], \quad (5)$$

where n is the layer number and $\Delta z = a_0/2$ is the distance between neighboring layers. The lattice constant for gold is $a_0 = 4.08$ Å.

One has to sum over an infinite number of layers, but Hentschke gives an example where the sum over 3 layers converges very quickly. A comparison of the wall potential, the layer potential and summation is plotted in Fig. 4.

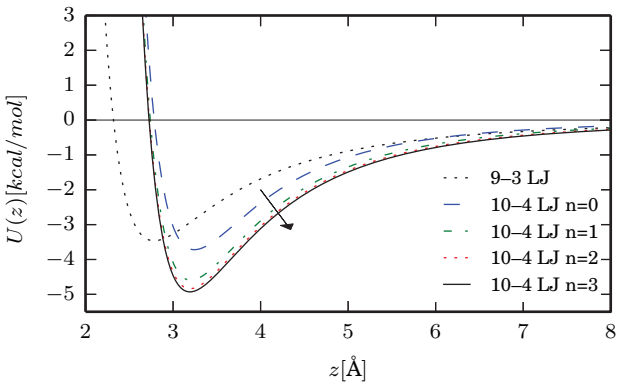

FIG. 4. Surface potential U_{surf} of an fcc crystal of Au particles interacting with a particle at a distance z from the surface. The potential U_{surf} is computed for a homogeneous crystal (9–3 LJ) and a crystal composed of $n + 1$ homogeneous layers (10–4 LJ) separated by a distance Δz.

We used the layered 10–4 LJ potential in this work. The height modulation of the top most layer of the reconstructed gold surface was modelled as

$$z(x) = z + \frac{\Delta h}{2}(1 - \cos\theta), \quad \theta = 2\pi\frac{x}{\lambda}. \quad (6)$$

The modulation amplitude $\Delta h = 0.7$ Å and wavelength $\lambda \approx 13.85$ Å were chosen to match the measured quantities.[14]

The final coarse-grained surface potential is

$$U_{\text{surf}}(z) = U_{\text{surf,10-4}}(z(x),0) + \sum_{n=1}^{3} U_{\text{surf,10-4}}(z,n). \quad (7)$$

The 12–6 LJ parameters $\epsilon_{\text{Au}} = 5.29$ kcal mol^{-1} and $\sigma_{\text{Au}} = 2.629$ Å for the gold atoms were taken from Heinz *et al.*[17] The atom number density of gold was computed to be $\rho = 0.059$ Å^{-3} at room temperature. We used atomistic 12–6 LJ parameters from Huang *et al.*[11] for the coarse-grained particles: S1 for P1, C4 for P2 and P3. Instead of the Lorentz-Berthelot rules we used the Waldman-Hagler rules,[18]

$$\sigma_{ij} = \left[\frac{1}{2}\left(\sigma_{ii}^6 + \sigma_{jj}^6\right)\right]^{1/6}, \quad (8)$$

$$\epsilon_{ij} = 2\sqrt{\epsilon_{ii}\epsilon_{jj}}\left(\frac{\sigma_{ii}^3\sigma_{jj}^3}{\sigma_{ii}^6 + \sigma_{jj}^6}\right), \quad (9)$$

to compute combined interaction parameters since they are known to produce better results for rare gases.

C. Monte Carlo simulations

In Monte Carlo simulations,[19–21] the thermodynamic behaviour of a system is investigated by preparing "random" states and calculating ensemble averages of quantities, rather than solving Newton's equations of motion as in molecular dynamics. These random states are generated by proposing certain updates (changes) to a conformation $\mathcal{C}$ of the system.

In 1953, Metropolis *et al.*[22] proposed what today is widely known as the Metropolis method. The probability of a state $\mathcal{C}$ of a system in the canonical ensemble is given by

$p(\mathcal{C}) \propto e^{-\beta E(\mathcal{C})}$, with $\beta = 1/k_B T$. To the system in state $\mathcal{C}$ with energy $E(\mathcal{C})$, an update is proposed to transform it into state $\mathcal{C}'$ with energy $E(\mathcal{C}')$. For a polymer system such an update could be the displacement of one monomer or the rotation of a part of the chain. The acceptance probability of a proposed update is given by $P(\mathcal{C} \to \mathcal{C}') = \min(1, e^{-\beta \Delta E})$, where $\Delta E = E(\mathcal{C}') - E(\mathcal{C})$. An update with $\Delta E \leq 0$ is always accepted. If $\Delta E > 0$, a random number $r \in [0, 1)$ is generated. Only if $r < e^{-\beta \Delta E}$ the update is accepted, otherwise it is rejected. A simulation with M measurements generates a time series for an observable $\mathcal{O}$. The mean value calculated from that time series is an estimate for the canonical expectation value of that observable, i.e., $\langle \mathcal{O} \rangle \approx \overline{\mathcal{O}} = \frac{1}{M} \sum_{i=1}^{M} \mathcal{O}_i$. (For an infinitely long simulation ($M \to \infty$): $\langle O \rangle = \overline{\mathcal{O}}$.)

The most basic Monte Carlo update for polymer systems is the displacement of a single particle: a particle is chosen at random and a random vector is added to its coordinates. The length of this vector can be tuned in the simulation to obtain a desired acceptance rate for this update. This is a local update and is close to the motion of particles in a realistic system. Due to its random nature, however, no real dynamics is sampled. More sophisticated update algorithms allow for faster equilibration and better sampling of the phase space. The pivot move,[23] for example, introduces a non-local update to the system, since a large part of the polymer is altered at once. The update goes as follows: a backbone particle (P1 particle) is chosen at random, a rotation axis at that point is selected at random and part of the chain is rotated about that axis. The shortest part of the chain was rotated to reduce the computational time. A further efficiency improvement was introduced by fixing the rotation axis to be perpendicular to the substrate. This results in a two-dimensional pivot update and allows for larger angles of rotation at the same acceptance rate. The latter is due to the strong adsorption of the polymer chain at the simulated temperature. In this case the three-dimensional pivot move proposes updates where parts of the chain either penetrate the substrate or leave it. Both are energetically unfavourable: the first is associated with an infinite energy, the second with a large energy increase. The last Monte Carlo update was a displacement of the whole molecule along the axis perpendicular to the substrate.

The polymer chain was initialised as a linear chain of particles P1. The side chains were alternating to the left and right of the backbone as depicted in Fig. 2. The molecule was placed parallel to the substrate at a distance of 4 Å.

IV. RESULTS

Figure 5(a) shows a typical room-temperature STM image of the Au(001) surface after *in situ* UHV electrospray deposition of individual P3HT molecules. In the image two terraces can be seen separated by a monoatomic step running from the upper center to the lower left corner of the image. On top of the terraces a closer look reveals a stripe-like modulation which results from the quasihexagonal reconstruction of the Au(001) surface.[14] This reconstruction induces two periodicities along orthogonal ⟨110⟩ high-symmetry directions: Narrow stripes with a spacing of 13.85 Å which

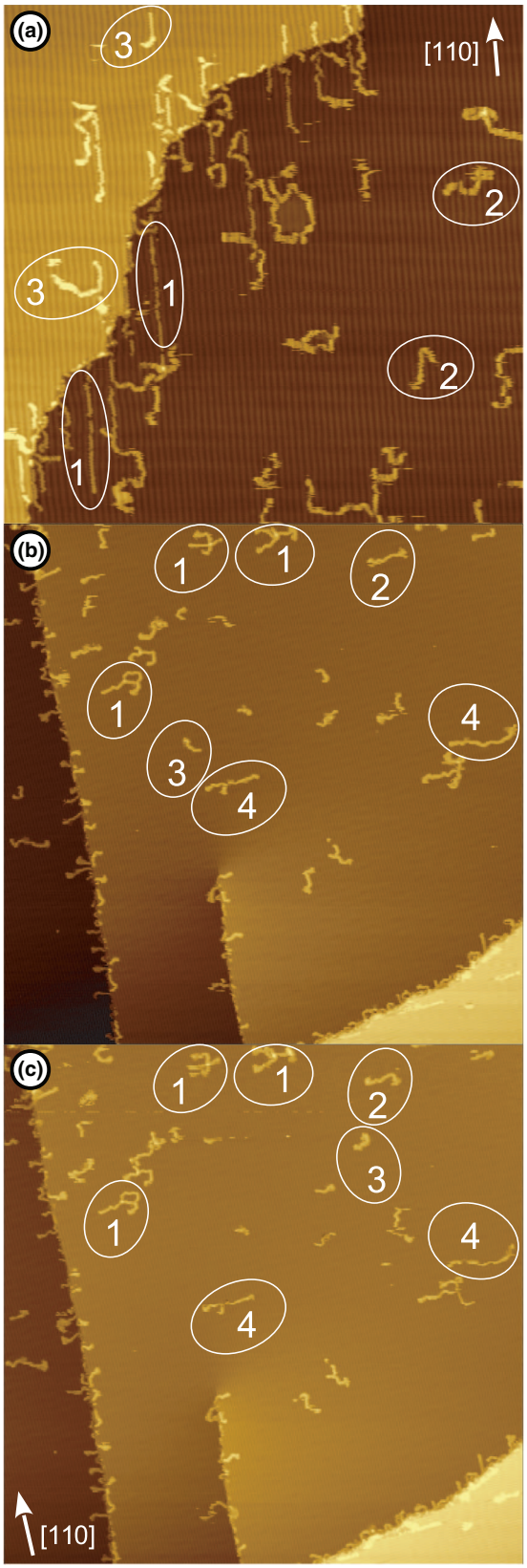

FIG. 5. STM images of *in situ* deposited P3HT molecules on the Au(001) surface. The images (b) and (c) are taken 15 min apart. For explanation see text. (a) 110 × 110 nm^2, 50 pA, −1.5 V. (b) and (c) 230 × 230 nm^2, 50 pA, −2.0 V.

corresponds to approximately five times the next-neighbor Au-Au distance. Additionally, an about four times larger periodicity is formed in the perpendicular direction. A

detailed description of the full c(48×24) reconstruction is presented elsewhere.[14] On top of the substrate terraces, a large number of individual P3HT molecules can be identified in Fig. 5(a). The chains are adsorbed on the substrate surface in a planar 2D geometry of the polymer backbone. The step edge in the image is fully decorated with polymer chains which indicates that this is the energetically most favourable adsorption site. This observation holds for the upper and the lower terrace side of the step edge. Moreover, molecules which are pinned at the steps can also extend across the steps on both terraces (not shown here). In addition to step-edge adsorption, P3HT molecules are also found in different adsorption geometries on the terraces. Some molecules are adsorbed in a fully stretched configuration aligned parallel to the narrow reconstruction rows of the substrate (marked by "1" in Fig. 5(a)). In contrast, a large fraction of the molecules adsorbs in a near random fashion (examples marked by "2"). Finally also a combination of both adsorption geometries can be observed. For some molecules only one part of the chain is stretched along the narrow trenches of the reconstruction whereas the remaining chain is crossing neighbouring rows with an irregular shape (marked by "3"). Previously we could show that the different adsorption geometries are related to different interaction strength of the polymer with the substrate.[10] The fully stretched chains are strongly interacting with the substrate. Their adsorption is accompanied with a lifting of the substrate reconstruction underneath. These molecules adsorb on locally unreconstructed, planar Au(001)-(1×1) areas. In contrast, the random configurations of the additional polymer chains indicate a weak polymer-substrate interaction.

The present work focusses on the statistical evaluation of the random-coil like 2D conformation of the weakly adsorbed P3HT molecules. Figures 5(b) and 5(c) show two subsequently recorded large-scale STM images measured at room temperature. The images show three substrate terraces separated by monoatomic steps. The first step runs straight from the top left corner to the bottom and the second step runs diagonally through the lower right part of the image. Additionally, a screw dislocation on the large central terrace can be seen which forms an additional step parallel to the first one. On the top-most terrace the stripe-like modulation is rotated by 90°. Here the second domain of the Au(001) surface reconstruction has formed. Besides step-edge adsorption, exclusively weakly adsorbed P3HT molecules are found with irregular shape on the large defect-free terraces. The chain lengths of the adsorbed P3HT molecules vary between 10 and 55 nm as determined with STM. This broad distribution allows to obtain statistical information for various lengths from a single deposition experiment. On the large terraces most P3HT molecules are well-separated from each other. However, some chains are crossing each other, e.g., the molecules marked by "1" in Figs. 5(b) and 5(c). The crossing point appears brighter in the STM images due to the increased height of the molecules at that point. These agglomerates formed from multiple chains remain stationary in subsequent STM images. In contrast, both images show that isolated molecules reveal a weak mobility leading to surface diffusion at room temperature. Some chains only partially changed their configuration within the time span of 15 min for recording the images, e.g., the molecule marked with "2". Other molecules diffuse over large distances as, e.g., the molecule marked with "3". Obviously different diffusion barriers exist. The diffusion rate might differ depending on the polymer lengths, but also the relative orientation of the chains with respect to the substrate seems to make a difference. Focussing on the orientation of the polymer chains relative to the substrate one notices that despite their irregular shape a large number of molecules is wiggling around a direction perpendicular to the narrow reconstruction rows. In this direction, the P3HT molecules experience a slight height modulation of the substrate surface. The wavelength of this modulation is approximately four times larger than the one of the narrow rows. In that orientation sometimes parts of molecules remain unchanged in subsequent measurements (see molecule marked by "2") but even full molecules are immobilized without being pinned at defects or crossings with other chains (see molecule marked by "4").

Besides the experimental observation of weakly adsorbed P3HT on the Au(001) surface in this work Monte Carlo simulations have been conducted at $T = 300$ K. The surface was coarse-grained as described in Sec. III B. The surface reconstruction was modelled as a wave-like modulation with spacing of 13.85 Å and an amplitude of 0.7 Å to mimic the strong modulation of the narrow reconstruction rows on the surface. However, the much weaker modulation in perpendicular direction is neglected. To obtain enough statistically relevant data the simulations were run for 10^7 Monte Carlo sweeps, after 10^6 sweeps to equilibrate all bond and torsion angles. Errors were calculated using the binning method.[24–26] For comparison with the experimental data only the single monomer displacement update was used during our simulations, since this update is close to a realistic particle movement on the surface. More advanced Monte Carlo updates, however, help to reach equilibrium states faster. The time scale to reach these equilibrium states in experiment is currently not precisely known.

Using the P3HT model as introduced in Sec. III A no influence of the height modulations of the reconstruction could be determined for the given parametrization of the interactions. Instead random chain configurations are observed which do not show any correlation to distinct substrate directions. This might be surprising since the periodicity of the narrow reconstruction rows of 13.85 Å nearly matches the next-neighbour distance of P3HT in molecular crystals of 14.1 Å.[27] But most likely the curvature of the surface is too strong to align weakly adsorbed P3HT along these rows. Only a planar substrate surface which can be obtained by lifting the reconstruction makes such an alignment favourable as observed for strongly adsorbed P3HT. That distinct ordering effects can be induced by a stripe-like pattern has recently been demonstrated within a generic polymer-adsorption model.[28] There the relative strength of the modulated surface attraction was varied systematically over a wide range.

When introducing the more advanced Monte Carlo updates described earlier, like pivot chain rotation, the simulations perfectly reproduce the complex configurations of adsorbed chains as observed with STM. In Fig. 6 two

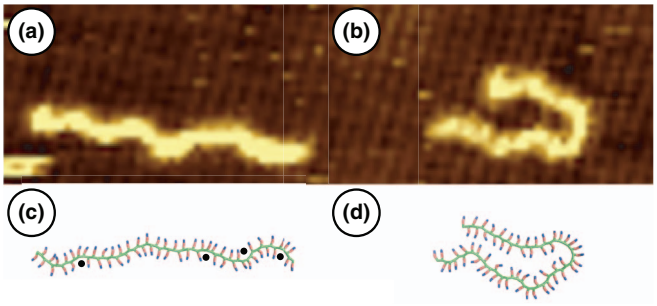

FIG. 6. Elongated coil ((a) and (c)), and collapsed hairpin conformations ((b) and (d)) of a 60 monomer chain as obtained in experiment (upper row) and simulation (lower row). Flipped side chains are marked with black dots in (c). (a) and (b) 25 × 14 nm^2, 50 pA, −2.0 V.

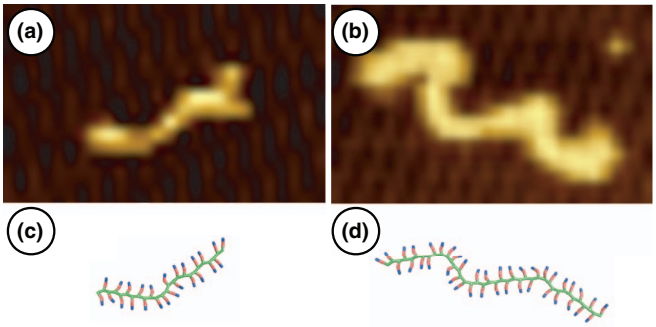

FIG. 7. Comparison of measured ((a) and (b)) and simulated conformations ((c) and (d)) of P3HT on Au(001) for molecules of identical length. ((a) and (b)) 16 × 10 nm^2, 50 pA, −2.0 V, ((a) and (c)) 25 monomer chain, and ((b) and (d)) 40 monomer chain.

characteristic conformations of a chain with a length of ∼60 monomer units are shown. The STM image in Fig. 6(a) shows an elongated slightly curved chain which makes seven turns. A comparable configuration taken from the simulation is shown in Fig. 6(c). All details of the conformation can be extracted from the simulated structure. As one can see, a small bending of the chain can arise from a local rearrangement of the side chains. However, a stronger curvature of the molecule is connected to a local *trans-cis* isomerization. The four black points along the chain in Fig. 6(c) mark the positions where single thiophene rings are flipped. This flip induces a bending of the chain. Additionally, an increased side chain density on one side of the backbone and the missing side chain on the other side can lead to further rearrangements which can give rise for an even stronger increase of the curvature. Figure 6(b) shows the same polymer chain in a different conformation recorded 45 min earlier. Here the chain exhibits a hairpin-like collapsed structure. As can be seen in the simulated hairpin-like conformation in Fig. 6(d), the full turn of the polymer chain results from a sequence of *trans-cis* isomerizations. However, this is only a single experimental event and the time scale of these structural fluctuations is not precisely known. The advantage of the more advanced Monte Carlo updates which have been used to compute the polymer conformations of Figs. 6(c) and 6(d) is that the equilibrium states can be reached faster. Interestingly the experimentally observed chain conformations are in good agreement with selected random chain conformations obtained from simulations despite the fact that in the simulations the substrate is strongly simplified and no geometrical constraint on the molecular orientation could be found. From the good agreements of the random chain configuration as derived from simulations with the experimentally observed chains one can conclude that although the molecules align in the experiment in a preferred direction they still have a sufficiently high degree of freedom to adopt random chain configurations.

Comparable results are obtained for different polymer lengths using only basic Monte Carlo updates. Results for chains with a length of 25 and 40 monomers are shown in Fig. 7. Qualitatively again a good matching of the measured and the simulated chain conformations can be obtained from the images. The computed images reveal in particular again the characteristic side chain flips.

For a quantitative description of the 2D polymer adsorption on Au(001) a statistical analysis of the detailed adsorption geometry for a large ensemble of individual P3HT molecules is necessary. For this purpose, we use a computer assisted tracing of individual polymer chains from STM data. This procedure determines the geometry of the polymer backbone and extracts the planar coordinates along the chain. Figure 8 illustrates the applied procedure using the molecule shown in Fig. 7(b). There the raw STM data of a single P3HT chain are shown with a resolution of 30×16 pixels. Although the STM image is of low resolution (since it is a section of a large-scale image covering a large number of individual and well-separated molecules as in Fig. 5), the chain geometry, marked as blue line, is well retrieved. This example demonstrates that a single large-scale STM measurement with relatively low resolution in the region of an individual molecule is sufficient to extract the full statistical information. This procedure allows recording simultaneously a large number of individual chains within a reasonable short time span (3–15 min).

In the following, we concentrate on two widely used quantities in polymer physics which can be calculated from the STM data. The radius of gyration R^2_{gyr} describes the dimensions of a polymer chain and its components R^2_{xx}, R^2_{yy}, and R^2_{zz} give the extensions of the chain along each axis:

$$R^2_{\mathrm{gyr}} = R^2_{xx} + R^2_{yy} + R^2_{zz} \tag{10}$$

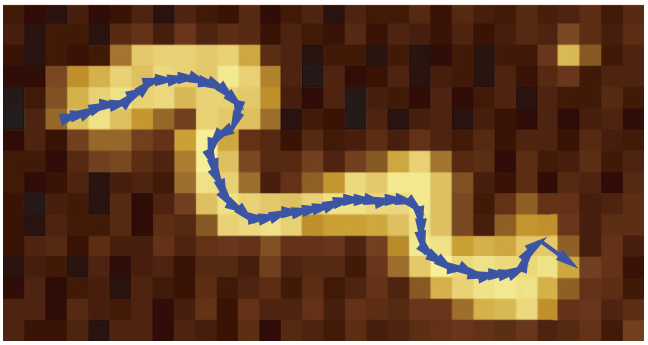

FIG. 8. Example for tracing P3HT polymers as measured with STM for extracting the statistical information. Raw data STM image, 30 × 16 px^2, 16.0 × 8.5 nm^2, 50 pA, −2.0 V,

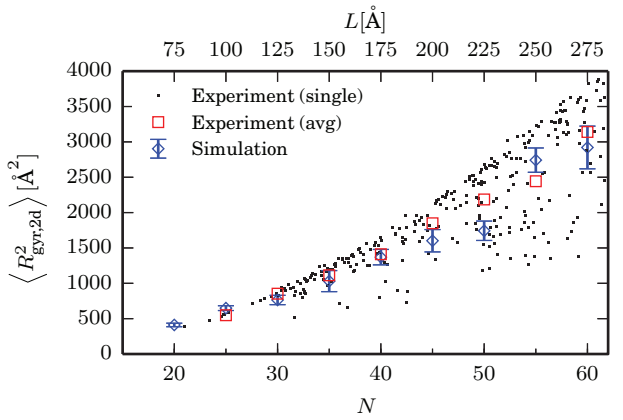

FIG. 9. Comparison of the two-dimensional radius of gyration obtained from experiment and simulation as a function of the monomer number N.

with

$$R^2_{ij} = \frac{1}{N}\sum_{n=1}^{N}\left(r_i^{(n)} - \bar{r}_i\right)\left(r_j^{(n)} - \bar{r}_j\right), \tag{11}$$

where N is the number of chain segments, $r_i^{(n)}$ $(i = x, y, z)$ is the ith Cartesian coordinate of the nth chain segment and $\bar{r}_i = \sum_{n=1}^{N} r_i^{(n)}/N$. For the 2D adsorption geometry of P3HT here, R^2_{zz} nearly vanishes and

$$R^2_{gyr} \approx R^2_{gyr,2d} = R^2_{xx} + R^2_{yy}. \tag{12}$$

The second characteristic quantity describing the chain extension is the end-to-end distance

$$R_{ee} = |\vec{r}_N - \vec{r}_1|. \tag{13}$$

The experimental and simulational data for $R^2_{gyr,2d}$ and for R_{ee} are plotted as functions of the polymer length N in Figs. 9 and 10, respectively. In both figures, the full set of experimentally determined data points is represented as small black squares. In total 230 chains have been extracted from the STM measurements. To give a statistical estimate of the mean and the standard deviation of an N-mer, the average over chains of length in the range from $N - 2$ to $N + 2$ is used. The simulational data were obtained from consecutively recorded structures every 1000 sweeps and add up to ten thousand conformations per data point. For the experimental (open red square) as well as for the simulation data (open blue diamonds) in Fig. 9, we find an almost linear increase of $R^2_{gyr,2d}$ with the chain length for $N \geq 35$. As we discuss below, this behaviour is related to a predominantly stretched geometry for the short chains. Random elongated coils as well as hairpin conformations were observed in the simulations for all chain lengths $N \geq 30$. However, elongated conformations are more likely to be found for shorter chains, whereas hairpins and collapsed chains are dominant for longer chains. Due to the resulting strong asymmetry in the distribution of the experimental values and the limited statistics a standard deviation of the mean is not given.

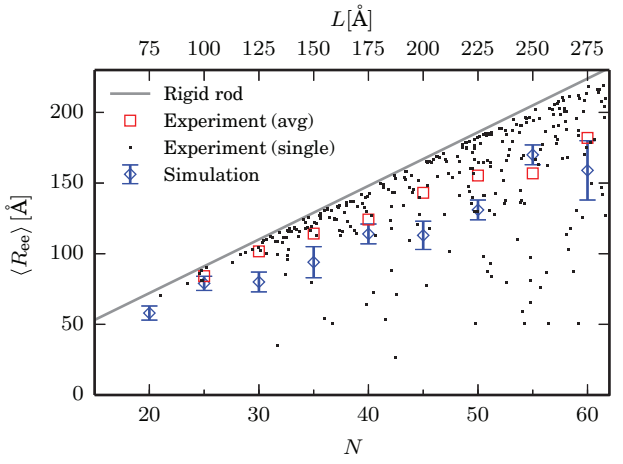

FIG. 10. Comparison of end-to-end distances obtained from experiment and simulation as a function of the monomer number N. The solid line indicates the linear $R_{ee} \sim (N - 1)$ dependence.

The second quantity to be discussed here is the average end-to-end distance of polymers of a given length. The experimental data as extracted from STM data are marked as full squares in Fig. 10 for polymer length in the range of 20 and 60 monomer units. Again, the polydispersity of the used P3HT sample allows to cover the wide length distribution within a single experiment. The gray line in the graph of Fig. 10 represents the theoretical end-to-end distance for rigid rod polymers. The length of a rigid rod of N monomers with a bond-length of $a = 3.828$ Å (the bond-length between particles P1) and a bending angle of $\alpha = 165^\circ$ is $L = a(N - 1)\sin(\alpha/2)$ and the end-to-end distance is $R_{ee} = L$.[29] Figure 10 shows that the end-to-end distance of most of the polymers linearly increases with increasing N with the same slope as for the ridig rod. Deviations from the rigid-rod description are due to *trans-cis* isomerizations within the chains, leading to a bending of the polymer backbone. As a consequence of this bending the end-to-end distances are decreased. The results in Fig. 10 show that short chains were mostly adsorbed in elongated conformations. However, with increasing chain length starting from $N \geq 30$ the P3HT molecules tend to adopt more strongly bended conformations. Focussing on the mean values of experiment and simulations this trend becomes obvious. The tendency of stronger bending for longer chains can also be well recognized from the inspection of large-scale STM images as shown in Fig. 5. As discussed above, the Monte Carlo simulations also quantitatively well describe the experimentally observed geometries up to $N = 60$.

V. SUMMARY

We showed that the behaviour of weakly adsorbed isolated P3HT chains on an Au(001) surface as observed with scanning tunneling microscopy can be well described with Monte Carlo simulations using this coarse-grained model. The STM data show two characteristic conformations of the adsorbed P3HT polymers, namely elongated chains and hairpins. These were reproduced using Monte Carlo simulations. Moreover, a good agreement between the experimental and simulational data of the end-to-end distance and radius of gyration of single polymer chains with a maximum length of 60 monomers was achieved. Our results show that the coarse-grained description of P3HT, neglecting the atomistic details

of the polymer, can be used to reflect the real behaviour of single molecules in computer simulations.

ACKNOWLEDGMENTS

Jens Balko and Thomas Thurn-Albrecht are acknowledged for assistance in P3HT preparation. The authors thank R. Kulla for technical support in setting up the ESD source. This work was supported by the Deutsche Forschungsgemeinschaft (DFG) in the framework of the SFB/TRR 102 "Polymers under multiple constraints."

[1]B. Xu and S. Holdcroft, Macromolecules **26**, 4457–4460 (1993).
[2]Z. Bao, A. Dodabalapur, and A. J. Lovinger, Appl. Phys. Lett. **69**, 4108 (1996).
[3]M. R. Andersson, O. Thomas, W. Mammo, M. Svensson, M. Theander, and O. Inganä, J. Mater. Chem. **9**, 1933 (1999).
[4]B. W. Boudouris, V. Ho, L. H. Jimison, M. F. Toney, A. Salleo, and R. A. Segalman, Macromolecules **44**, 6653–6658 (2011).
[5]J. M. Frost, F. Cheynis, S. M. Tuladhar, and J. Nelson, Nano Lett. **6**, 1674 (2006).
[6]M. Campoy-Quiles, T. Ferenczi, T. Agostinelli, P. G. Etchegoin, Y. Kim, T. D. Anthopoulos, P. N. Stavrinou, D. D. C. Bradley, and J. Nelson, Nat. Mater. **7**, 158 (2008).
[7]A. M. Ballantyne, L. Chen, J. Dane, T. Hammant, F. M. Braun, M. Heeney, W. Duffy, I. McCulloch, D. D. C. Bradley, and J. Nelson, Adv. Funct. Mater. **18**, 2373 (2008).
[8]Z.-Y. Yang, H.-M. Zhang, G.-B. Pan, and L.-J. Wan, ACS Nano **2**, 743 (2008).
[9]Y.-F. Liu, K. Krug, and Y. L. Lee, Nanoscale **5**, 7936 (2013).
[10]S. Förster and W. Widdra, J. Chem. Phys. **141**, 054713 (2014).
[11]D. M. Huang, R. Faller, K. Do, and A. J. Moule, J. Chem. Theory Comput. **6**, 526 (2010).
[12]C. J. Satterley, L. M. Perdigao, A. Saywell, G. Magnano, A. Rienzo, L. C. Mayor, V. R. Dhanak, P. H. Beton, and J. N. O'Shea, Nanotechnology **18**, 455304 (2007).
[13]A. Saywell, G. Magnano, C. J. Satterley, L. M. Perdigao, N. R. Champness, P. H. Beton, and J. N. O'Shea, J. Phys. Chem. C **112**, 7706 (2008).
[14]R. Hammer, A. Höfer, S. Förster, M. Kiel, K. Meinel, and W. Widdra, Phys. Rev. B **90**, 035446 (2014).
[15]W. A. Steele, Surf. Sci. **36**, 317 (1973).
[16]R. Hentschke, Macromol. Theory Simul. **6**, 287 (1997).
[17]H. Heinz, R. A. Vaia, B. L. Farmer, and R. R. Naik, J. Phys. Chem. C **112**, 17281 (2008).
[18]M. Waldman and A. T. Hagler, J. Comput. Chem. **14**, 1077 (1993).
[19]W. Janke, "Monte Carlo simulations in statistical physics: From basic principles to advanced applications," in *Order, Disorder and Criticality: Advanced Problems of Phase Transition Theory*, Vol. 3, edited by Y. Holovatch (World Scientific, Singapore, 2012), pp. 93–166.
[20]D. P. Landau and K. Binder, *A Guide to Monte Carlo Simulations in Statistical Physics*, 3rd ed. (Cambridge University Press, New York, 2009).
[21]M. E. J. Newman and G. T. Barkema, *Monte Carlo Methods in Statistical Physics* (Clarendon Press, Oxford, 1999).
[22]N. Metropolis, A. W. Rosenbluth, M. N. Rosenbluth, A. H. Teller, and E. Teller, J. Chem. Phys. **21**, 1087 (1953).
[23]N. Madras and D. Sokal, J. Stat. Phys. **50**, 109 (1988).
[24]W. Janke, in *Proceedings of the Euro Winter School Quantum Simulations of Complex Many-Body Systems: From Theory to Algorithms*, NIC Series Vol. 10, edited by J. Grotendorst, D. Marx, and A. Muramatsu (John von Neumann Institute for Computing, Jülich, 2002), p. 423.
[25]D. P. Landau, Phys. Rev. B **13**, 2997 (1976).
[26]W. W. Wood, *Physics of Simple Liquids* (Wiley, New York, 1968).
[27]X. Ma, Y. Guo, T. Wang, and Z. Su, J. Chem. Phys. **139**, 014701 (2013).
[28]M. Möddel, W. Janke, and M. Bachmann, Phys. Rev. Lett. **112**, 148303 (2014).
[29]The ridgid-rod line for the experimental values would be shifted by the length of one monomer to higher end-to-end distances since the experimental chain length includes the extension of the monomers at both ends of the chain, whereas the monomers are treated as point-like objects in the calculations.